Concentration measurement of gas embedded in scattering media by employing absorption and time-resolved laser spectroscopy

Gabriel Somesfalean, Mikael Sjöholm, Janis Alnis, Claes af Klinteberg, Stefan Andersson-Engels, and Sune Svanberg

Diode-laser-based absorption spectroscopy for the evaluation of embedded gas concentrations in porous materials is demonstrated in measurements of molecular oxygen dispersed throughout scattering polystyrene foam, used here as a generic test material. The mean path length of light scattered in the material is determined with the temporal characteristics of the radiation transmitted through the sample. This combined with sensitive gas-absorption measurements employing wavelength-modulation spectroscopy yields an oxygen concentration in polystyrene foam of 20.4% corresponding to a foam porosity of 98%, which is consistent with manufacturing specifications. This feasibility study opens many possibilities for quantitative measurements by using the method of gas-in-scattering-media absorption spectroscopy.

OCIS codes: 290.7050, 300.1030, 290.4210, 300.6380, 300.6390.

1. Introduction

Embedded gas is often found in porous materials of both organic and synthetic origin. Monitoring the distributed free gas can convey the internal gas concentration, pressure, and temperature and can reveal useful information about the bulk material, e.g., internal structure and diffusion characteristics. Recently, we demonstrated a new technique, called gas in scattering media absorption spectroscopy (GASMAS),[1] used for the characterization and diagnostics of free gas in scattering solids and turbid liquids. Initial demonstrations included proof-of-principle measurements of the embedded oxygen concentration relative to an equivalent column of air and of the internal gas pressure as well as assessment of the gas exchange. We analyzed the dispersed gas *in situ* by using absorption spectroscopy, employing a single-mode probing diode laser tuned over a sharp absorption feature of the free gas molecule. The absorption and scattering cross sections of the bulk material display slow wavelength dependence; thus these properties can be assumed to be constant over the wavelength range tuned. Wavelength modulation techniques[2] are used to increase the detection sensitivity and to discriminate effectively against background signals, allowing for detection of around 10^{-4}–10^{-5} absorption fractions of the light received.

Owing to inhomogeneities on the microscopic scale in the optical properties of the turbid medium, the radiation is scattered multiple times in the material. This prevents a straightforward application of the Beer–Lambert law, which requires well-defined path lengths. However, using a temporally resolved technique, as is routinely done in tissue optics studies,[3,4] a mean path length of the diffused light can be estimated, which together with the strength of the gas absorption determines the concentration of the dispersed gas. In this paper we demonstrate the possibility of quantitative concentration measurements by using polystyrene foam as a generic test material.

2. Theoretical Background

To extract the concentration of gas embedded in a turbid sample, we employ two independent measurements to obtain the gas absorbance a and the absorption path length L, respectively. The Beer–Lambert law yields the transmitted intensity over a free path length L of a species with a concentration

The authors are with the Department of Physics, Lund Institute of Technology, P.O. Box 118, Lund, Sweden. S. Svanberg can be reached at sune.svanberg@fysik.lth.se.

Received 23 July 2001; revised manuscript received 2 January 2002.

0003-6935/02/183538-07$15.00/0

c and a wavelength-dependent absorption cross section $\sigma(\lambda)$ according to

$$I(\lambda) = I_0(\lambda)\exp[-\sigma(\lambda)cL] = I_0(\lambda)\exp(-a), \quad (1)$$

where $I_0(\lambda)$ is the initial injected intensity and $I(\lambda)$ is the recorded intensity of the transmitted light. One obtains the gas absorbance using Eq. (1) by measuring the transmitted intensity through the sample at wavelengths on and off the gas absorption line. The expression cL can thus be determined from the transmission measurement, assuming that the absorption cross section is known. The optical path length in a scattering medium L_{sm} is, however, not simply the thickness of the sample but is determined by the absorption and scattering properties of the material as well as by measurement geometry. Independent measurements of both the absorbance and the optical path length are thus necessary to obtain the concentration. The absorption of the gas is often small compared with the bulk material absorption, and will thus essentially not influence the optical path length. The influence of gas absorption on the optical path length is neglected below.

The absorption path length can be estimated as the mean path length traveled by the photons $\langle l \rangle$. Two different approaches can be used to determine the path length, by a direct time-resolved measurement or indirectly by assessing the optical properties of the medium, making it possible to calculate L_{sm} with the use of a transport model for the light propagation within the sample. In the limit of small absorptions the mean traveled path length can be estimated from the experimentally determined average time of flight of the photons $\langle t \rangle$ according to

$$L_{\mathrm{sm}} = \langle l \rangle = v\langle t \rangle, \quad (2)$$

where v is the velocity of light in the scattering material. The material optical properties can be assessed experimentally in three different ways: by time-resolved, spatially resolved, and frequency-domain measurements.

In this research the powerful technique of time-resolved measurements utilizing ultrashort light pulses and fast optical detection was used for studying photon propagation in multiple-scattering materials.[3,4] The analysis of the time-resolved data was based on the diffusion approximation to the radiative-transfer theory. When solving the diffusion equation, one must specify the boundary conditions. In the case of simple geometries, such as a slab with finite thickness and infinite expansion, the most common approach is to mirror an infinite set of imaginary positive and negative isotropic sources in an extrapolated boundary at some distance beyond the actual surface, to insure that the fluence rate of photons is fully canceled. It yields an analytic expression for the transmitted pulse shape in terms of the absorption coefficient μ_a and the reduced scattering coefficient μ_s' of the sample material. In the case of an infinitely extended slab of scattering material the time-dependent transmitted intensity can be expressed as[5]

$$\begin{aligned} I(\rho, d, t) = {} & (4\pi Dv)^{-3/2}\, t^{-5/2} \\ & \times \exp\left(-\mu_a v t - \frac{\rho^2}{4Dvt}\right) \\ & \times \sum_{k=0}^{+\infty} \left[z_{-k} \exp\left(-\frac{r_{-k}^{\,2}}{4Dvt}\right) \right. \\ & \left. - z_{+k} \exp\left(-\frac{r_{+k}^{\,2}}{4Dvt}\right) \right], \end{aligned} \quad (3)$$

where ρ is the lateral injection–detection separation, d is the slab thickness, $D = [3(\mu_a + \mu_s')]^{-1}$ is the diffusion coefficient, $z_0 = (\mu_s')^{-1}$ is the mean free path of isotropic scattering, $z_{\pm k} = (2k + 1)d \pm z_0$ is the depth of the imaginary sources used to fulfill the boundary conditions, and $r_{\pm k} = (\rho^2 + z_{\pm k}^{\,2})^{1/2}$ is the distance between the detector position and the sources used in the calculations. One can evaluate the optical properties of a sample by fitting such an analytical expression to the experimentally acquired temporal dispersion curve by adjusting the free parameters: the absorption, and reduced scattering coefficients. For a slab of thickness d the expression for the average time of flight of the photons, calculated by integration of Eq. (3), is given by[6]

$$\langle t \rangle = \frac{\sum_{k=0}^{\infty} \left[\frac{z_{+k}}{r_{+k}} \exp(-\mu_{\mathrm{eff}} r_{+k}) - \frac{z_{-k}}{r_{-k}} \exp(-\mu_{\mathrm{eff}} r_{-k}) \right]}{2vD \sum_{k=0}^{\infty} \left[\frac{z_{+k}}{r_{+k}^{\,3}} (1 + \mu_{\mathrm{eff}} r_{+k}) \exp(-\mu_{\mathrm{eff}} r_{+k}) - \frac{z_{-k}}{r_{-k}^{\,3}} (1 + \mu_{\mathrm{eff}} r_{-k}) \exp(-\mu_{\mathrm{eff}} r_{-k}) \right]}, \quad (4)$$

where $\mu_{\mathrm{eff}} = (\mu_a/D)^{1/2}$ is the effective attenuation coefficient. If the distribution of gas in the porous material is assumed to be homogeneous and the absorption is of the order of a few percent, the detected gas absorption signal can be considered the integrated contribution from all exiting photons. A typical theoretical time-dispersed curve for light transmitted through a 39-mm-thick sample with the optical parameters $\mu_a = 0.002\ \mathrm{cm}^{-1}$ and $\mu_s' = 40\ \mathrm{cm}^{-1}$ is shown in Fig. 1. The broad time-of-flight distribution of the photons, corresponding to the absorption path lengths through the embedded

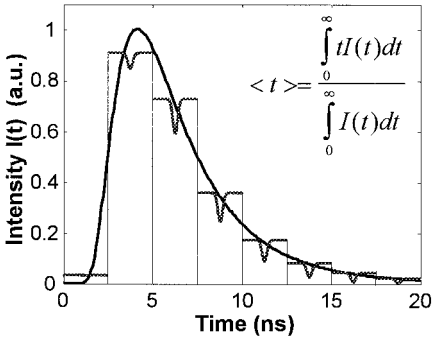

Fig. 1. Analytical time dispersion curve obtained for transillumination of a 39-mm-thick slab with optical parameters $\mu_a = 0.002$ cm^{-1} and $\mu_s' = 40$ cm^{-1} by using short-pulsed light. For clarity the direct absorption signals corresponding to photons that have traveled distances of different lengths in the material are intentionally exaggerated. The mean traveling time in the limit of small absorptions is shown in the inset.

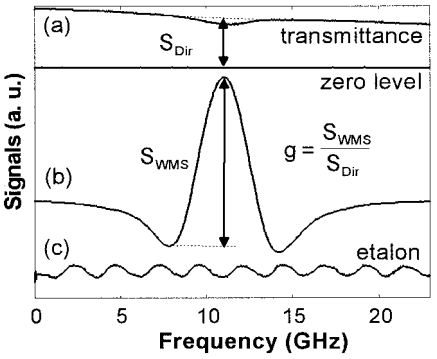

Fig. 2. (a) Direct absorption and (b) second-harmonic component of the WMS spectrum for the R7R7 line in the oxygen A band measured along a 10-m-long path in air. (c) Low-finesse fringes from a 2.43-GHz free spectral range Fabry–Perot etalon used for calibration of the frequency scale.

gas, gives rise to varying absorption signal strengths, which are also schematically shown in Fig. 1. Thus the gas absorption can be used as a means to track the history of the photons in the material.

A simpler alternative to the time-resolved measurement technique, also explored in the present research, is to use a cw laser source and to spatially monitor the diffuse light-intensity distribution at the sample surface.[7,8] When the recorded light intensity is plotted versus, e.g., the injection–detection separation distance, the final slope of the curve at large distances is found to be determined by the effective attenuation coefficient μ_{eff}. The spatially resolved measurement method also requires that the absolute intensities of the injected and scattered light be measured, which may be difficult to perform experimentally because of unknown conditions regarding the coupling of light at the medium boundary. Solving the diffusion equation in the steady-state case yields a transmitted intensity for an infinite slab of scattering material:

$$I(\rho, d) = \frac{1}{2\pi} \sum_{k=0}^{\infty} \left[\frac{z_{-k}}{r_{-k}^3} (1 + \mu_{eff} r_{-k}) \exp(-\mu_{eff} r_{-k}) - \frac{z_{+k}}{r_{+k}^3} (1 + \mu_{eff} r_{+k}) \exp(-\mu_{eff} r_{+k}) \right]. \quad (5)$$

In our previous research on measurements of molecular oxygen,[1] we expressed the concentration of the gas in a scattering medium by introducing an equivalent mean path length L_{eq}. It is defined as the distance traversed by light in air, yielding a detected signal of the same magnitude as that from the absorption of photons by oxygen embedded in the porous material according to

$$c_{air} L_{eq} = c_{sm} L_{sm}, \quad (6)$$

where c_{air} is the oxygen concentration in air and c_{sm} is the oxygen concentration in the scattering medium. The purpose of the present paper is to demonstrate quantitative gas concentration measurements. Thus determination of an effective absorption path length can be performed by means of time-resolved and spatially resolved measurements.

3. Experiment

The experimental setup for GASMAS measurements has been described in detail.[1] Basic experiments of the GASMAS type are conveniently performed on molecular oxygen, because this gas is normally diffused from the surrounding atmosphere into porous materials. A near-IR single-mode diode laser (Sharp LT031MDO) was placed in a nitrogen-flushed chamber, and the light was brought to the sample through a 0.6-mm-core-diameter optical fiber to ensure that the ambient air did not influence the measurements. A transilluminating geometry was chosen, in that the samples were placed on a long-pass colored-glass filter (Schott RG 695) attached directly to the cathode surface of a photomultiplier tube 2 in. (~50 mm) in diameter (EMI 9558 QA). A very high sensitivity and a large dynamic range were achieved with this detector setup, which is necessary when only small and variable amounts of light seep through the scattering materials under observation. In the measurements performed in this study, relatively high transmitted light intensities were available, and it was thus possible to spatially limit the detection area by using a mask with a circular aperture 3 mm in diameter. Thus spatially resolved measurements could also be performed.

The experiments were performed on the strong, isolated R7R7 line at 761.003 nm in the oxygen A band. Wavelength-modulation spectroscopy (WMS) employing lock-in techniques was used to pick up the second-harmonic component, which produces a signal similar to the second derivative of the original absorption line shape. An experimental signal for oxygen in free air is shown in Fig. 2, where a direct absorption recording is also included. In our case modulation at 55 kHz (Philips PM5139) effectively discriminated the background signals by shifting the

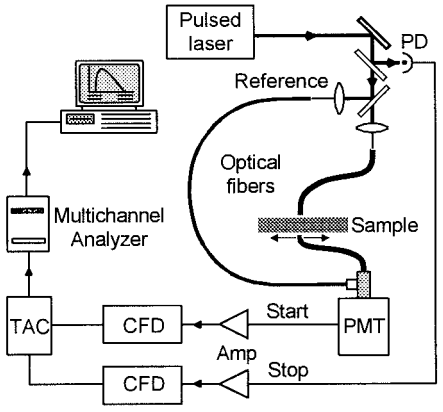

Fig. 3. Experimental setup used for time-resolved measurements: PD, photodiode; PMT, photomultiplier tube; Amp, amplifier; CFD, constant fraction discriminator; TAC, time-to-amplitude converter.

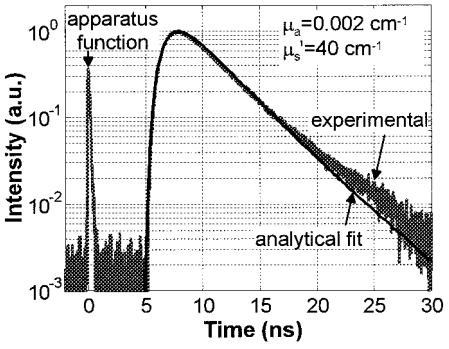

Fig. 4. Recorded time dispersion curve obtained when transilluminating a 39-mm-thick slab of polystyrene foam by using a diode laser source pulsed at 10 MHz. A fit of a theoretical curve and the instrumental transfer function are also depicted.

detection band to a high-frequency region where the noise level is low.[2] An absolute absorption calibration was established by performing a long-path measurement in free atmosphere, where the direct absorption signal could also be observed. Curves (a) and (b) in Fig. 2 are recordings obtained for a 10-m-long absorption path length in air. To compensate for variations in the detected light intensity, the experimental WMS signal S_{WMS} was normalized against the interpolated intensity of the diffused light at the line center S_{Dir}, defining a GASMAS differential absorption signal

$$g \equiv \frac{S_{\mathrm{WMS}}}{S_{\mathrm{Dir}}}, \tag{7}$$

determined for the selected modulation parameters. The Fabry–Perot etalon fringes in Fig. 2(c) allow the oxygen linewidth to be evaluated to ~3.6 GHz.

Figure 3 shows a schematic diagram of the experimental setup used for the time-resolved measurements. Two different laser sources were used for generation of picosecond-long light pulses: a diode laser with a repetition rate of 10 MHz (Mitsubishi ML4405 with a Bios Quant DL4040 driver) and a mode-locked Ti:Sapphire laser with a repetition frequency of 76 MHz (Coherent MIRA 900). Diode lasers are particularly convenient to use in such applications because of their simple operation, compact size, and ability to produce short light pulses when high-frequency components are applied to the driving current. The average output power of the diode laser was less than 1 mW, while only a small fraction of the available radiation of the Ti:Sapphire laser was used. Both lasers were tuned near the selected absorption wavelength of oxygen around 761 nm. Owing to the broadened linewidths of the short-pulsed lasers and low gas absorption, the gas has no significant influence on the photon propagation through the scattering medium. A transillumination arrangement was used, as shown in Fig. 3, although a backscattering detection scheme can in certain cases be more appropriate. Optical fibers with a core diameter of 0.6 mm were employed for light injection and for collection of scattered radiation, with the samples placed between the fiber ends. The injector–detector separation could be varied by translating the collecting fiber. The transmitted light was detected with a microchannel plate photomultiplier tube (Hamamatsu R2566U-07), which ensured high detection sensitivity. The time-correlated single-photon detection technique was employed, including a constant fraction discriminator, a time-to-amplitude converter TAC, and a multichannel analyzer.[4,9] The photon arrival time distribution was recorded, and the overall temporal response function of the system was ~140 ps for the diode laser and ~60 ps for the Ti:Sapphire laser. The latter number corresponds essentially to the electronic response time, since the Ti:Sapphire laser has a subpicosecond pulse length.

Spatially resolved gas absorption measurements of GASMAS type combined with transmitted light intensity measurements were also performed with transilluminating geometry. The incident beam diameter was 3 mm, and the receiving photomultiplier tube, with a detection area masked down to 3 mm in diameter, could be translated sideways.

The measurements were performed on polystyrene foam samples of different thicknesses but of the same kind. We have chosen polystyrene foam as a model scattering material, owing to its relatively high homogeneity, strong scattering properties, and high gas content, i.e., factors that contribute to a strong gas signature. This material also has a great industrial and commercial importance since it is extensively used as an insulation and packaging material.

4. Results

Figure 4 shows the recorded photon-arrival-time distribution curve for a 39-mm-thick slab of polystyrene foam measured with the diode laser. The time response of the system itself, the apparatus function, was obtained at time $t = 0$ by using a separate fiber, transmitting part of the laser pulse directly to the detector (see Fig. 3). This signal also provided a

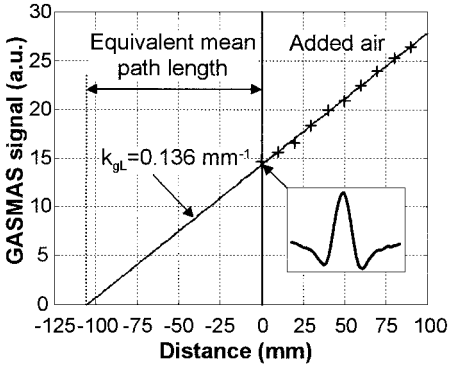

Fig. 5. Standard-addition plot for molecular oxygen obtained with the GASMAS setup showing the extrapolated equivalent mean path length for a 9.4-mm-thick slab of polystyrene foam. The WMS signal obtained with the light-injecting collimator in direct contact with the sample is shown in the inset.

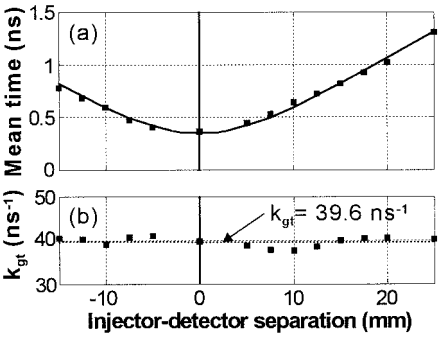

Fig. 6. (a) Recorded mean time of flight through a 9.4-mm-thick slab of polystyrene foam measured with a pulsed Ti:Sapphire laser. Solid curve, theoretical curve corresponding to the evaluated optical parameters (μ_a = 0.002 cm^{-1}, μ_s' = 40 cm^{-1}). (b) Dotted line, quotient between the GASMAS signal and the mean traveling time of the photons together with a least-squares fit of the factor k_{gt}.

time reference during the measurement. As can be seen from the time distribution curve, a certain fraction of the photons has traveled more than 15 ns through the material, i.e., corresponding to a path length of 4.5 m, although the physical thickness of the slab is only 0.039 m. The absorption and scattering coefficients of the polystyrene foam were determined by first convolving the solution of the diffusion equation, Eq. (3), to the impulse response of the system and then fitting the resulting curve to the detected time dispersion curve, as shown in Fig. 4. Note that the scale is logarithmic, causing small discrepancies in the low-intensity region at late times to be clearly visible. No extrapolated boundary condition was employed in the model owing to the resulting negligible corrections. In principle, laser-induced fluorescence could perturb the measurements. However, because of the long excitation wavelength, the fluorescence is negligible compared with the directly scattered light. The evaluated absorption coefficient is μ_a = 0.002 cm^{-1}, and the transport scattering coefficient is μ_s' = 40 cm^{-1}, yielding an effective attenuation coefficient μ_{eff} = 0.5 cm^{-1}.

Gas-absorption spectroscopy data for a 9.4-mm-thick slab of polystyrene foam embedded with atmospheric oxygen are shown in Fig. 5. It illustrates the amplitude variation of the GASMAS signal for several added free columns of air and is used to estimate an extrapolated equivalent mean path length in polystyrene foam according to the standard-addition method. Since the fraction of light absorbed by the gas within the medium is small, corresponding to only a few percent of the incident light, the absorption signal g is approximately linearly proportional to the concentration. We denote the slope of the curve

$$k_{gL} \equiv \frac{g}{L}, \tag{8}$$

where L is the absorption path length in air. The oxygen concentration in the polystyrene foam can now be estimated as

$$c_{\text{sm}} = \frac{c_{\text{air}} L_{\text{eq}}}{v\langle t\rangle} = \frac{g}{\langle t\rangle}\frac{c_{\text{air}}}{v k_{gL}}, \tag{9}$$

where Eqs. (2) and (6) and substitution of $L = L_{\text{eq}}$ in Eq. (8) have been utilized. To minimize the influence of material inhomogeneities, temporal dispersion curves were also recorded for various lateral positions of the detector. The pulsed Ti:Sapphire laser was employed in such a measurement on a 9.4-mm-thick polystyrene foam slab. An experimental plot of the directly evaluated mean photon arrival time versus various injector–detector separations is shown in Fig. 6(a), derived from these measurements. A theoretical curve corresponding to the evaluated optical parameters is also plotted according to Eq. (4). In Fig. 6(b) the experimental value at different injection–detection separations of the ratio between the GASMAS signal and the mean time of flight, $k_{gt} \equiv g/\langle t\rangle$, is shown together with a least-squares fit. The uncertainty in the ratio was 1.3%, evaluated by using a 95% confidence interval of the experimental values. The only unknown factor left is the index of refraction of the scattering material n_{sm}, which determines the light velocity in the medium according to $v = c_0/n_{\text{sm}}$ where c_0 is the light velocity in vacuum. Owing to the homogeneous and isotropic nature of the porous material, the macroscopic index of refraction was estimated as a weighted mean of the refractive indices of the individual compounds contained, i.e.,

$$n_{\text{sm}} = P n_{\text{air}} + (1 - P) n_b, \tag{10}$$

where P is the material porosity, n_{air} and n_b are the indices of refraction of air and of the bulk material, respectively. In the case of gas equilibrium with the surrounding atmosphere we can derive the foam po-

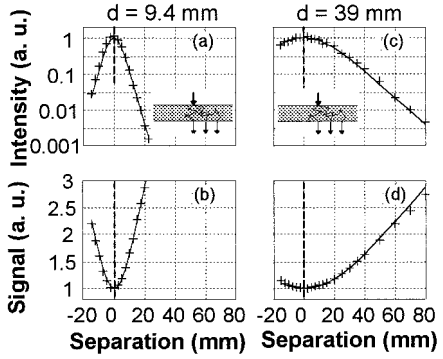

Fig. 7. Spatially resolved transmission recordings measured with the GASMAS setup on two polystyrene foam slabs (a), (b) 9.4 mm and (c), (d) 39 mm thick: upper curves, transmitted intensity; lower curves, detected oxygen absorption signal amplitude for different injector–detector separation distances. Fits according to the evaluated effective attenuation coefficient ($\mu_{\text{eff}} = 0.5\ \text{cm}^{-1}$) are also indicated. A schematic of the transillumination setup is shown in the insets, and dashed lines at the zero position mark the symmetry axis.

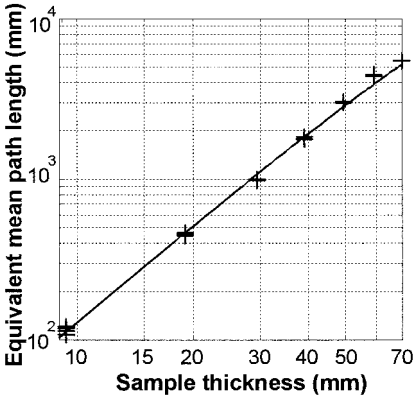

Fig. 8. Plot of the equivalent mean path length corresponding to oxygen absorption measured through slabs of polystyrene foam with different thicknesses by using a diode laser. The mean time of flight is proportional to the square of the slab thickness. Solid line, theoretical curve evaluated with $\mu_a = 0.002\ \text{cm}^{-1}$ and $\mu_s' = 40\ \text{cm}^{-1}$.

rosity P from the embedded gas concentration by using

$$P = \frac{V_{\text{gas}}}{V_{\text{tot}}} = \frac{c_{\text{sm}}}{c_{\text{air}}}, \tag{11}$$

where V_{gas} is the volume of gas in the porous material and V_{tot} is the total volume of the porous material. With an index of refraction of the polystyrene bulk material, $n_b = 1.4$, and an atmospheric oxygen content of 20.8%, the oxygen concentration in the polystyrene foam can be evaluated accordingly with Eqs. (9)–(11) to yield $c_{\text{sm}} \approx 20.4\%$ and the corresponding foam porosity $P \approx 98\%$.

The mean time of flight of the photons, and consequently the embedded gas concentration, can as described above also be evaluated indirectly by spatially resolved measurement techniques. Experimental curves recorded with the GASMAS setup are shown for a 9.4-mm-thick [Figs. 7(a), 7(b)], and a 39-mm-thick [Figs. 7(c), 7(d)] slab of polystyrene foam. Figures 7(a) and 7(c) show the total transmitted light intensity as a function of lateral displacement, where the zero separation corresponds to the position where the injector and the detector are placed opposite to each other. Figures 7(b) and 7(d) display the GASMAS signal of the embedded oxygen. Note that the transmitted light intensity falls off laterally as the GASMAS signal increases. The distributions are, as expected, broader in the case of the thicker slab. The experimental points are plotted in Fig. 7 together with theoretical curves [Eqs. (4) and (5)] where the effective attenuation coefficient evaluated above is used. In the general case the mean time of flight can thus be evaluated when we insert the obtained optical parameters into the analytical formula, Eq. (4). However, a fit of the theoretical curve to the spatially resolved steady-state data measured at long injection–detection separation ($\rho \gg z_0$) can provide only an unambiguous value for the lumped coefficient μ_{eff} and not for μ_a and μ_s' separately. The embedded gas concentration can thus not readily be assessed by using only these kinds of steady-state measurements.

Measurements on polystyrene foam slabs of different thicknesses were also performed, and the variation in the equivalent mean path length with the slab thickness is plotted in Fig. 8. It can be seen in Fig. 8 that in the case of polystyrene foam, which has weak absorption and strong scattering properties, the mean time of flight related to the equivalent mean path length is proportional to the square of the thickness of the slab, i.e., $\langle t \rangle \propto d^2$, as predicted by Eq. (4) for the case of low gas absorption. A similar relationship was also obtained by considering the related topic of light propagation through clouds.[10]

5. Conclusions and Discussions

We have shown that the embedded gas concentration can be estimated by using time-resolved measurements together with the newly developed GASMAS technique. The proof-of-principle measurements were performed on atmospheric oxygen at a wavelength characterized by weak absorption. The gas was embedded in polystyrene foam, which is a model material with high porosity and strong scattering properties. The evaluated porosity of polystyrene foam is comparable with manufacturing specifications. However, in the more general case of moderate porosity or of substantial gas absorption, it is still a subject for further investigation whether there is any preference for the photons to travel through the diffused gas or through the bulk material when being multiply scattered inside the porous material. This is a research topic that might reveal novel insights into the field of light propagation through confining media.

Note that some aspects of the GASMAS technique

do not require detailed knowledge about light propagation, as in the present case of an absolute concentration measurement. For example, gas pressure, temperature, and ratios between gas concentrations are quantities that can be readily evaluated, being largely independent of light scattering inside the porous medium.

Gas tomography is another possible application of the technique. This extension corresponds to the one done for optical mammography and skull hematoma detection.

An alternative to the time and spatially resolved techniques presented in this paper is to perform phase-sensitive measurements in the frequency domain.[11,12] A major advantage of such a method is that it needs only one single diode laser both for the GASMAS measurements and for determination of optical properties of the bulk material by using modulation techniques.

This research was supported by the Swedish Research Council for Engineering Sciences (TFR), the Knut and Alice Wallenberg Foundation, and the Swedish Institute.

References

1. M. Sjöholm, G. Somesfalean, J. Alnis, S. Andersson-Engels, and S. Svanberg, "Analysis of gas dispersed in scattering media," Opt. Lett. **26,** 16–18 (2001).
2. U. Gustafsson, G. Somesfalean, J. Alnis, and S. Svanberg, "Frequency-modulation spectroscopy with blue diode lasers," Appl. Opt. **39,** 3774–3780 (2000).
3. B. Chance, J. S. Leigh, H. Miyake, D. S. Smith, S. Nioka, R. Greenfeld, M. Finander, K. Kaufmann, W. Levy, M. Young, P. Cohen, H. Yoshioka, and R. Boretsky, "Comparison of time-resolved and unresolved measurements of deoxyhemoglobin in the brain," Proc. Natl. Acad. Sci. USA **85,** 4971–4975 (1988).
4. S. Andersson-Engels, R. Berg, S. Svanberg, and O. Jarlman, "Time-resolved transillumination for medical diagnostics," Opt. Lett. **15,** 1179–1181 (1990).
5. M. S. Pattersson, B. Chance, and B. C. Wilson, "Time-resolved reflectance and transmittance for the noninvasive measurement of tissue optical properties," Appl. Opt. **28,** 2331–2336 (1989).
6. S. R. Arridge, M. Cope, and D. T. Delpy, "The theoretical basis for the determination of optical path lengths in tissue: temporal and frequency analysis, "Phys. Med. Biol. **37,** 1531–1560 (1992).
7. T. J. Farrell, M. S. Pattersson, and B. Wilson, "A diffusion theory model of spatially resolved, steady-state diffuse reflectance for noninvasive determination of tissue optical properties *in vivo,*" Med. Phys. **19,** 879–888 (1992).
8. J. S. Dam, P. E. Andersen, T. Dalgaard, and P. E Fabricius, "Determination of tissue optical properties from diffuse reflectance profiles by multivariate calibration," Appl. Opt. **37,** 772–778 (1998).
9. R. Berg, O. Jarlman, and S. Svanberg, "Medical transillumination imaging using short-pulsed diode laser," Appl. Opt. **32,** 574–579 (1993).
10. U. Platt, Institute for Environmental Physic, University of Heidelberg, Heidelberg, Germany (personal communication, 2000).
11. J. K. Link, "Measurements of the radiative lifetimes of the first excited states of Na, K, Rb, and Cs by means of the phase shift method," J. Opt. Soc. Am. **56,** 1195–1199 (1966).
12. J. B. Fishkin, E. Gratton, M. J. Vande Ven, and W. W. Mantulin, "Diffusion of intensity-modulated near-infrared light in turbid media," in *Time-Resolved Spectroscopy and Imaging of Tissues*, B. Chance and A. Katzir, eds., Proc. SPIE **1431,** 122–135 (1991).